Supporting Information

Coupling FeNi Alloys and Hollow Nitrogen-Enriched Carbon Framework Leads to High-Performance Oxygen Electrocatalysis for Rechargeable Zinc-Air Battery

Haihong Wu,[†a,b] Min Zeng,[†a] Zhiyun Li,[†a] Xiang Zhu,[*,c]

Chengcheng Tian,[d] Chungu Xia,[*,a] Lin He[*,a] and Sheng Dai[d]

H. H. Wu, Dr. M. Zeng, Z. Y. Li, Prof. C. G. Xia, Prof. L. He

[a] State Key Laboratory for Oxo Synthesis and Selective Oxidation, Suzhou Research Institute of Lanzhou Institute of Chemical Physics (LICP), Chinese Academy of Sciences, Lanzhou, 730000, China

[*] Email: cgxia@licp.cas.cn; helin@licp.cas.cn

H.H. Wu

[b] University of Chinese Academy of Sciences, Beijing, 100049, China

Dr. X. Zhu

[c] Department of Chemistry, Texas A&M University, College Station, Texas, 77843, USA

[*] Email: xiang@tamu.edu/zhuxiang.ecust@gmail.com

Dr. C. Tian, Prof. S. Dai

[d] Chemical Sciences Division, Oak Ridge National Laboratory, Oak Ridge, TN 37831, USA

[†] These authors contributed equally to this work

Experimental Section

Preparation of FeNi/GS and FeNi/HNC. 30 ml of 25 mM Nickel acetate solution was added dropwise into 20 ml of 25 mM $K_3[Fe(CN)_6]$ solution under magnetic stirring. The pH of the final solution was adjusted to pH = 1 with diluted HCl solution. Then the solution was heated at 80 °C for 20 h in an electric oven.[1] After the reaction was completed, solid precipitates were collected by centrifugation, repetitively washed in distilled water, and lyophilized. This yielded blackish green-colored PB-FeNi.

To prepare **FeNi/GS**, PB-FeNi was annealed in Ar at different temperatures from 500-700 °C for 1 h.

To prepare **FeNi/HNC**, as-annealed **FeNi/GS** powders were further treated with 1 M HCl for 8 hours. Controlled samples with different etching times (4 and 16 hours) were also prepared for comparison. The final product was then collected, washed with a copious amount of distilled water and finally lyophilized.

Characterizations. SEM images were taken from Zeiss scanning electron microscope. TEM and STEM were carried on an FEI Tecnai F20 transmission electron microscope at an accelerate voltage of 200 kV. XRD was performed on PANalytical X-ray diffractometer. XPS spectra were collected on SSI S-Probe XPS Spectrometer. ICP-AES measurements were conducted on Varian Vista MPX. Samples were first calcined in air at 600 °C for 30 min, then digested in concentrated HNO_3 and diluted to desired concentrations. TGA analyses of powder samples were conducted on Mettler Toledo TGA/DSC1 Simultaneous Thermal Analyser in Ar. The temperature was programmed to rise from 25 °C to 800 °C at 10 °C min^{-1}. Raman spectrum of powder samples were recorded on LabRAM HR Raman microscope with a laser excitation wavelength of 514 nm. The nitrogen adsorption and desorption isotherm was measured at 77 K using a Micromeritics ASAP 2020 surface area analyzer.

Electrochemical measurements.

To ensure its accuracy and reproducibility, the Hg/HgO reference electrode was carefully calibrated against reversible hydrogen electrode (RHE) in 1 M KOH (Fig. S13). All the potentials were recorded with respect to the Hg/HgO and were conversed to RHE in the paper through the equation: $E_{(vs\ RHE)} = E_{(vs\ Hg/HgO)} + 0.922$. For ORR experiments, 1 mg of **FeNi/GS** or **FeNi/HNC** powder was mixed with 0.5 mg of Ketjenblack and 10 μl of 5 wt% Nafion solution, and dispersed in 0.25 ml of ethanol with the assistance of at least 40 min sonication to form a homogeneous ink. Then the catalyst ink was dropcast onto the glassy carbon disk (diameter 5.6 mm) of a rotation ring disk electrode (RRDE) to achieve a catalyst loading from 0.1 mg cm^{-2} to 0.4 mg cm^{-2}. Commercial 20 wt% platinum supported on Vulcan carbon black was purchased from FuelCellStore, and was measured alongside with **FeNi/GS** and **FeNi/HNC**. The catalyst ink was prepared by dispersing 3 mg of Pt/C or Ir/C and 24 μL of 5 wt% Nafion solution in 1.0 ml of ethanol under sonication for 40 min, then Pt/C or Ir/C catalyst ink was droped onto glassy carbon disk of a RRDE to achieve a catalyst loading of 0.3 mg cm^{-2}. RRDE voltammetry was carried out in 1 M KOH solution under the control of CHI 760 bipotentiostat. Hg/HgO and a graphite rod were used as the reference and counter electrode, respectively. Potentials were recorded with respect to Hg/HgO and then converted to RHE in the paper. Prior to the start of each measurement, the electrolyte was bubbled with O_2 for > 30 min. A flow of O_2 was then maintained over the electrolyte surface during the measurement in order to keep its continued O_2 saturation. The scan rate for RRDE polarization curves was 10 mV s^{-1}. For the analysis of peroxide yield, the ring potential was held constant at 1.2 V vs. RHE. The percent of H_2O_2 and the number of electron transfer (n) were determined by the following equations:

$$\%(H_2O_2) = 200 \cdot \frac{I_r/N}{I_d + I_r/N}; \qquad n = 4 \cdot \frac{I_d}{I_d + I_r/N}$$

where I_d is the disk current, I_r is the ring current, and N (N= 0.37) is the current collection efficiency of the Pt ring.

The Faradaic efficiency ε for OER was calculated using the following equation:

$$\varepsilon = \frac{I_r}{I_d * S}$$

Where I_r is the collected ring current, I_d is the disk current of 200 μA, and S is the current collection efficiency (I_r=42.6 μA, S=21.3 %) for OER, which has been determined using IrO_2 catalyst in film electrode.[2, 3]

For primary Zn-air battery tests, 1 mg of **FeNi/HNC** or 20 wt% Pt/C was mixed with 0.5 mg of Ketjen black and 10 μl of 5 wt% Nafion solution, and dispersed in 0.25 ml of ethanol with the assistance of at least 40 min sonication to form a homogeneous ink. This catalyst ink was uniformly dropcast onto 1 cm^2 of hydrophobic carbon paper electrode to achieve a catalyst loading of 1 mg cm^{-2}. The air cathode was then paired with a Zn foil anode, and assembled in a customized electrochemical cell filled with 6 M KOH. Polarization data (*V-i*) were collected using linear sweep voltammetry at a scan rate of 10 mV s^{-1} with its impedance corrected to R = 1 Ω for consistency throughout the experiment. Chronopotentiometry (*i-t*) data were manually corrected to R = 1 Ω. For rechargeable Zn-air battery tests, the electrolyte was 6 M KOH with 0.2 M zinc acetate solution. Discharge and charge polarization curves were measured by CHI 760E. Discharge–charge cycling were performed at room temperature using the double-pulse method, where one cycle consisted of a discharging step (10 mA cm^{-2} for 1 hour) followed by a charging step with the same current and duration time.

Table S1. A brief survey of OER activity for reported high-performance nonprecious material.[4-21]

Reference	Catalysts	Electrolyte	Loading (μg cm^{-2})	E_{j10} (V vs. RHE)
This work	**FeNi@HNC**	**1 M KOH**	**300 μg cm^{-2}**	**1.48**
Nanoscale, **2016**, 8, 20048-20055.[4]	CoFe@NCNTs	0.1 M KOH	800 μg cm^{-2}	1.68
*ACS Catal., **2017**,* 7, 469–479.[5]	FeCoNi@NG	1 M KOH	1000 μg cm^{-2}	1.56
Adv. Energy Mater. **2016**, 1601555.[6]	$Cu_{0.3}Co_{2.7}P$/NC	1 M KOH	400 μg cm^{-2}	1.42
J. Am. Chem. Soc. **2016**, 138, 10226-10231.[7]	Co_4N/CNW/CC	1 M KOH	N/A	1.54
*ACS Appl. Mater. Interfaces, **2016**, 8,* 34396–34404.[8]	FeNi/$NiFe_2O_4$@NC	1 M KOH	131 μg cm^{-2}	1.55
Energy Environ. Sci. **2016**, 9, 123-129.[9]	FeNi@NG	1 M NaOH	N/A	1.51
Electrochimica Acta **2016**, 220, 354-362.[10]	FeCo@NG	1 M KOH	400 μg cm^{-2}	1.49
Angew. Chem. Int. Ed. 2018 DOI:10.1002/anie.201803136.[11]	Fe-Ni@NC-CNTs	1 M KOH	500 μg cm^{-2}	1.50
Energy Environ. Sci. **2014**, 7, 609–616.[12]	N-CG–CoO	1 M KOH	708 μg cm^{-2}	1.57
Angew. Chem. Int. Ed. **2014***,* 53, 8508–8512.[13]	Ni_xO_y/NC	0.1 M KOH	210 μg cm^{-2}	1.64
Adv. Mater. **2017**, 1703185.[14]	Co/N/O tri-doped graphene (NGM-Co)	0.1 M KOH	250 μg cm^{-2}	1.72
Angew. Chem. Int. Ed. **2017**, 56, 610-614.[15]	S,N-Fe/N/C-CNT	0.1 M KOH	600 μg cm^{-2}	1.60
Adv. Funct. Mater. **2017**, 1700795.[16]	CoZn-NC-700	0.1 M KOH	240 μg cm^{-2}	1.62
Adv. Energy Mater. **2016***,* 1601172.[17]	Ni_3Fe/N-C sheets	0.1 M KOH	130 μg cm^{-2}	1.60
Adv. Mater. **2017**, 1702526.[18]	$CoO_{0.87}S_{0.13}$/GN	0.1 M KOH	360 μg cm^{-2}	1.59
Adv. Mater. **2017**, 1701410.[19]	$Fe_{0.5}Co_{0.5}O_x$/NrGO	1 M KOH	500 μg cm^{-2}	1.49
Nano letter **2016**, 16, 6516-6522.[20]	NiCo/PFC	0.1 M KOH	130 μg cm^{-2}	1.53
Energy Environ. Sci. **2015**, 8, 2347-2351.[21]	Ni_2P nanoparticles	1 M KOH	140 μg cm^{-2}	1.51

Table S2. A brief survey of ORR activity for reported promising nonprecious material.[1, 7, 10, 15-17, 19, 22-38]

Reference	Catalysts	Electrolyte	Loading (μg cm^{-2})	$E_{1/2}$ (V vs. RHE)
This work	**FeNi@HNC**	**1 M KOH**	**300 μg cm^{-2}**	**0.87**
Adv. Funct. Mater. **2016**, 26, 4397-4404.[1]	Co@NG-acid	1 M KOH	470 μg cm^{-2}	0.83
Angew. Chem., Int. Ed. **2013**, *52*, 371-375.[22]	Pod-Fe@CNT	1 M NaOH	380 μg cm^{-2}	0.79
J. Mater. Chem. A **2016**, *4*, 1694-1701.[23]	Co/N-CNTs	0.1 M KOH	200 μg cm^{-2}	0.84
ACS Nano **2015**, *9*, 6493-6501.[24]	Fe/N-CNTs	0.1 M KOH	200 μg cm^{-2}	0.81
ACS Nano **2015**, *9*, 6493-6501.[24]	CuFe@carbon	0.1 M KOH	390 μg cm^{-2}	0.85
Chem. Eur. J. **2015**, *21*, 14022-14029.[25]	Co@NBCNT	0.1 M KOH	880 μg cm^{-2}	0.81
Green Chem. **2016**, *18*, 427-432.[27]	Co_3C-GNRs	0.1 M KOH	140 μg cm^{-2}	0.77
Green Chem. **2016**, *18*, 427-432.[27]	Ni_3C-GNRs	0.1 M KOH	140 μg cm^{-2}	0.77
Green Chem. **2016**, *18*, 427-432.[27]	Fe/Fe_3C@HG	0.1 M KOH	140 μg cm^{-2}	0.71
Adv. Energy Mater. **2014**, *4*, 1400337.[28]	N-doped Fe/Fe_3C@C	0.1 M KOH	710 μg cm^{-2}	0.83
Angew. Chem., Int. Ed. **2015**, *54*, 8179-8183.[29]	Fe_3C@Fe-N-CNF	0.1 M KOH	600 μg cm^{-2}	0.83
Nature Nanotechnology **2015***,* 10, 444–452.[30]	N and P co-doped mesoporous nanocarbon (NPMC)	0.1 M KOH	150 μg cm^{-2}	0.85
J. Am. Chem. Soc. **2016**, 138, 10226-10231.[7]	Co_4N/CNW/CC	1 M KOH	N/A	0.80
Electrochimica Acta, **2016**, 220, 354-362.[10]	FeCo@NG	0.1 M KOH	400 μg cm^{-2}	0.80
J. Am. Chem. Soc. **2015***,* 137, 1436-1439.[31]	Hollow Spheres of FeC@NG	0.1 M KOH	1200 μg cm^{-2}	0.80
J. Am. Chem. Soc. **2016**, 138, 3570–3578.[32]	Fe@C‐FeNC	0.1 M KOH	700 μg cm^{-2}	0.90
Adv. Funct. Mater. **2015**, 25, 872–882.[33]	N/Co-doped PCP//NRGO	0.1 M KOH	714 μg cm^{-2}	0.87
ACS Nano. **2015***,* 9, 7407-7418.[26]	Fe_3C-GNRs	0.1 M KOH	142 μg cm^{-2}	0.78
ACS Nano. **2015***,* 9, 7407-7418.[26]	Co_3C-GNRs	0.1 M KOH	142 μg cm^{-2}	0.77
ACS Nano. **2015***,* 9, 7407-7418.[26]	Ni_3C-GNRs	0.1 M KOH	142 μg cm^{-2}	0.77
Advanced Materials **2015**, 27, 2521-2527.[34]	Fe_3C/NG-800	0.1 M KOH	400 μg cm^{-2}	0.86
Angew. Chem. Int. Ed. **2014**, 53, 3675–3679.[35]	Fe_3C/C	0.1 M KOH	600 μg cm^{-2}	0.83
Angew. Chem. Int. Ed. **2017**, 56, 610-614.[15]	S, N-Fe/N/C-CNT	0.1 M KOH	600 μg cm^{-2}	0.85

Adv. Funct. Mater. **2017**, 1700795.[16]	CoZn-NC-700	0.1 M KOH	240 μg cm^{-2}	0.84
Adv. Energy Mater. **2016**, 1601172.[17]	Ni_3Fe/N-C sheets	0.1 M KOH	130μg cm^{-2}	0.78
Adv. Mater. **2017**, 1701410.[19]	$Fe_{0.5}Co_{0.5}O_x$/NrGO	1 M KOH	500μg cm^{-2}	0.83
Angew.Chem.Int. Ed. **2016**, 55, 4087–4091.[36]	Co@Co_3O_4/NC	0.1 M kOH	210 μg cm^{-2}	0.80
Angew.Chem.Int. Ed. **2015**, 54, 9654-9658.[37]	NCNT/CoO-NiO-NiCo	1 M kOH	210 μg cm^{-2}	0.83
Nano Energy **2015**, *13*, 387-396.[38]	Fe@N–C-700	0.1 M KOH	311 μg cm^{-2}	0.83

Table S3. A brief survey of the potential difference between OER and ORR ($\Delta E = E_{OER@10\ mA/cm2} - E_{1/2-ORR}$) for the reported non-precious material in rechargeable Zn-air battery.[7, 13, 16, 17, 20, 23, 36, 38-43]

Reference	Catalysts	Electrolyte	$E_{1/2}$ (V vs. RHE)	$E_{j=10}$ (V vs. RHE)	ΔE (V)
This work	**FeNi@HNC**	**1 M KOH**	**0.87**	**1.48**	**0.61**
	Pt/C	1 M KOH	0.90	1.87	0.97
	Ir/C	1 M KOH	0.84	1.51	0.67
Adv. Energy Mater. **2017**, 7, 1601172.[17]	Ni_3Fe/N-C sheets	0.1 M KOH	0.86	1.62	0.84
ACS Appl. Mater. Interfaces. **2017**, 9, 5213-5221.[39]	Fe/N/C@BMZIF	0.1 M KOH	0.85	1.64	0.79
Nano Lett. **2016**, 16, 6516-6522.[20]	NiCo/PFC	0.1 M KOH	0.79	1.65	0.86
ACS Appl. Mater. Interfaces. **2017**, 9, 21216-21224.[40]	$Fe_3C/Co(Fe)O_x$@N CNT	0.1 M KOH	0.86	1.58	0.72
Nano Energy, **2015**, 13, 387-396.[38]	Fe@N-C-700	0.1 M KOH	0.83	1.71	0.88
Nano Energy, **2016**, 30, 801-809.[41]	PFSA-$Fe_{3.5}Ni$	0.1 M KOH	0.85	1.64	0.79
Angew. Chem. Int. Ed. **2014**, 5, 8508-8512.[13]	Co_xO_y/NC	0.1 M KOH	0.71	1.66	0.95
Nanoscale **2014**, 6, 15080-15089.[42]	Co/N-C-800	0.1 M KOH	0.74	1.60	0.86
Small **2014**, 10, 2251-2259.[43]	N-Doped Graphene/CNT	0.1 M KOH	0.73	1.77	1.04
Angew.Chem.Int. Ed. 2016, 55,4087–4091.[36]	Co@Co_3O_4/NC	0.1 M KOH	0.8	1.65	0.85
J. Am. Chem. Soc. 2016, 138, 10226–10231.[7]	Co_4N/CNW/CC	1 M KOH	0.8	1.54	0.74
Adv. Funct. Mater. 2017, 1700795.[16]	CoZn-NC-700	0.1 M KOH	0.84	1.62	0.78
J. Mater. Chem. A, **2016**, 4, 1694-1701.[23]	Co/N-CNTs	0.1 M KOH	0.84	1.62	0.78

Table S4. A brief survey of primary Zn-air batteries with key parameters.[1, 10, 14-16, 24, 38, 41, 44-53]

Reference	Catalysts	Loading (mg cm^{-2})	Current Density @ 1.0 V (mA cm^{-2})	Maximum Power Density (mW cm^{-2})
This work	**FeNi/HNC**	**1.0**	**215**	**310**
Adv. Funct. Mater. 2016, 26, 4397-4404.[1]	Co@NG-acid	1.0	255	350
Nature Commun. **2013**, *4*, 1805.[44]	CoO/N-CNT	1.0	197	265
Energy, Environ. Sci. **2011**, *4*, 4148-4154.[45]	Graphene supported Mn_3O_4 nanoparticles	N/A	70	120
Nano Lett. **2011**, *11*, 5362-5366.[46]	Ketjenblack carbon supported amorphous MnO_x	N/A	120	190
Electrochim. Acta **2011**, *56*, 5080-5084.[47]	N-doped carbon nanotubes	2.0	50	75
J. Power Sources **2011**, *196*, 3673-3677.[48]	Fe, Co and N precursors pyrolyzed with carbon	1.5	150	232
Nano Energy **2015**, *13*, 387-396.[38]	Fe@N–C-700	2.2	157	220
ACS Nano **2015**, *9*, 6493-6501.[24]	FeCu@GC	N/A	100	212
Nano Energy, **2016**, 30, 801-809.[41]	PFSA-$Fe_{3.5}$Ni	2.35	197.4	262
J. Power Sources, **2013**, 243, 267-273.[49]	N-doped porous carbon nanofibers	2.0	150	194
Adv. Mater. **2017**, 1703185.[14]	Co/N/O tri-doped graphene (NGM-Co)	1.5	80	150
Angew. Chem. Int. Ed. **2017**, 56, 610-614.[15]	S,N-Fe/N/C-CNT	4.0	~70	102.7
Nano Energy, **2017**, 37, 98-107.[50]	NCNT array	N/A	160	190
Adv. Funct. Mater. **2017**, 1700795.[16]	CoZn-NC-700	1.2	87	100
Nano Energy, **2017**, 31, 541-550.[51]	$NiCo_2S_4$/N-CNT	1.0	107	147
Adv. Mater. **2016**, 28, 3000–3006.[52]	Nanoporous carbon fiber films (NCNF)	2.0	150	185
ACS Nano **2017**, 11, 347−357.[53]	P,S-CNS	N/A	85	198
Electrochimica Acta, **2016**, 220, 354-362.[10]	FeCo@NG	1.0	70	132

Table S5. A brief summary of rechargeable Zn-air batteries performance of **FeNi/HNC** with various catalysts.[14, 16, 18-20, 37, 44, 50, 51, 54, 55]

Reference	Catalysts	Charge and Discharge Current Density (mA cm^{-2})	Charge and Discharge Voltage Gap (V)	Voltaic Efficiency
This work	**FeNi/HNC**	10	0.69	64.7%
Nano letter **2016**, 16, 6516-6522.[20]	NiCo/PFC	10	0.64	65.4%
Angew. Chem. Int. Ed. **2017**, 56, 9901-9905.[54]	Fe_3Pt/Ni_3FeN	10	0.74	58.6%
Nano Energy, **2017**, 37, 98-107.[50]	NCNT array	10	0.75	62%
Angew.Chem.Int. Ed. **2015**, 54, 9654-9658.[37]	NCNT/CoO-NiO-NiCo	20	0.86	~57%
Adv. Mater. **2017**, 1701410.[19]	$Fe_{0.5}Co_{0.5}O_x$/NrGO	10	0.79	62.6%
Nano Energy, 2016, 20, 315-325.[55]	NCNT/$Co_xMn_{1-x}O$	7.0	0.57	64.8%
Adv. Mater. **2017**, 1702526.[18]	$CoO_{0.87}S_{0.13}$/GN	20	0.76	64.4%
Nature Commun. **2013**, *4*, 1805.[44]	CoO/N-CNT	20	~0.70	65%
Adv. Mater. **2017**, 1703185.[14]	Co/N/O tri-doped graphene (NGM-Co)	1.0	0.7	63%
Adv. Funct. Mater. **2017**, 1700795.[16]	CoZn-NC-700	10	0.73	63%
Nano Energy, **2017**, 31, 541-550.[51]	$NiCo_2S_4$/N-CNT	10	0.69	67.2%

Table S6. Atomic and mass ratios of Fe, Ni, C and N mearsured from EDX.

Etching time (h)	Content	Fe	Ni	C	N
0	Atom.%	9.3	13.4	71.2	6.1
	Wt.%	23.1	35.1	38.0	3.8
4	Atom.%	5.4	7.8	81.3	5.5
	Wt.%	16.7	25.3	53.8	4.2
8	Atom.%	2.9	4.0	88.7	4.4
	Wt.%	10.6	15.4	70.0	4.0
16	Atom.%	1.9	2.7	91.5	3.9
	Wt.%	7.5	11.2	77.5	3.8

Figures

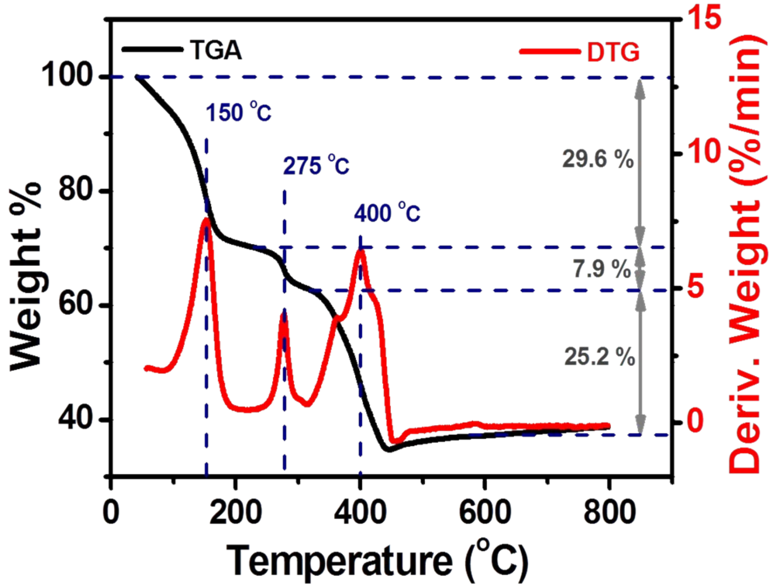

Figure S1. TGA (black) and its corresponding first order differential curve (red) of **PB-FeNi** under Ar.

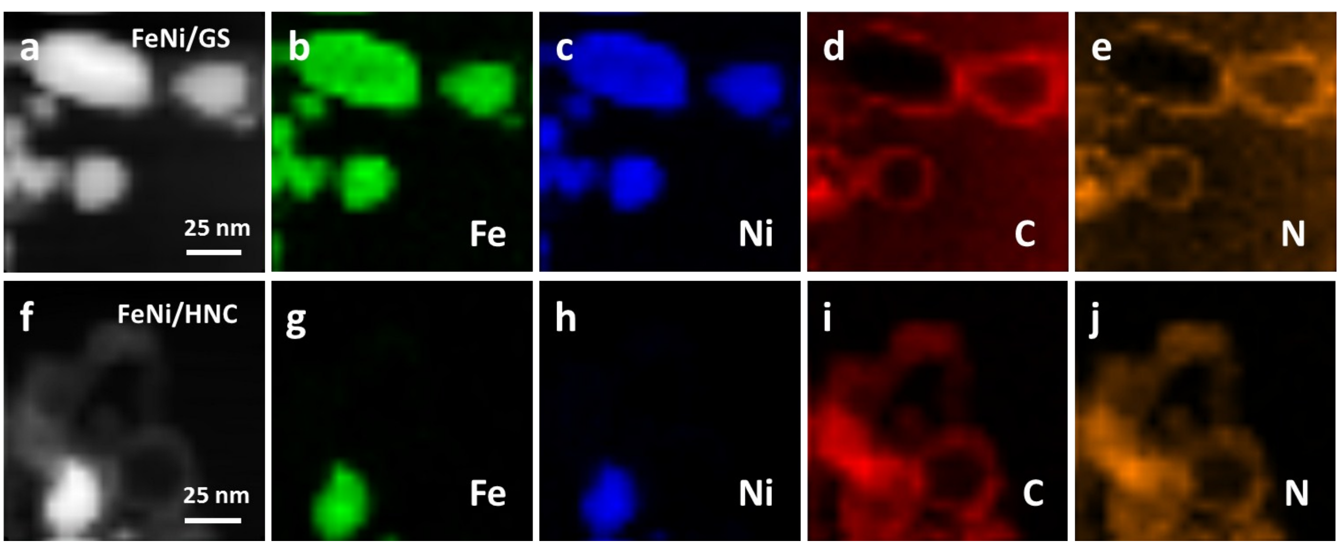

Figure S2. STEM image and corresponding Fe, Ni, C, N EDS elemental mapping of (a-e) **FeNi/GS** and (f-j) **FeNi/HNC**.

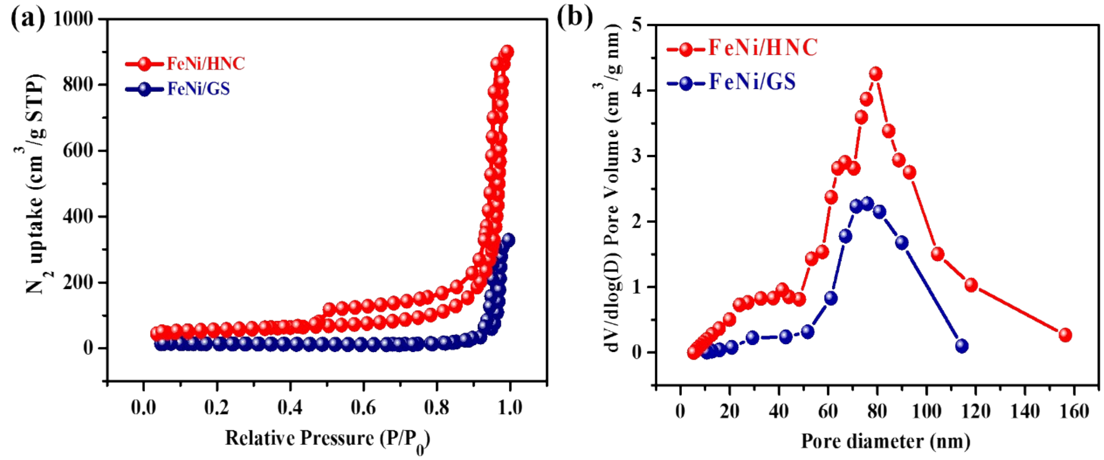

Figure S3. N_2 adsorption-desorption isotherms (a) and pore size distribution of **FeNi/HNC** and **FeNi/GS** (b).

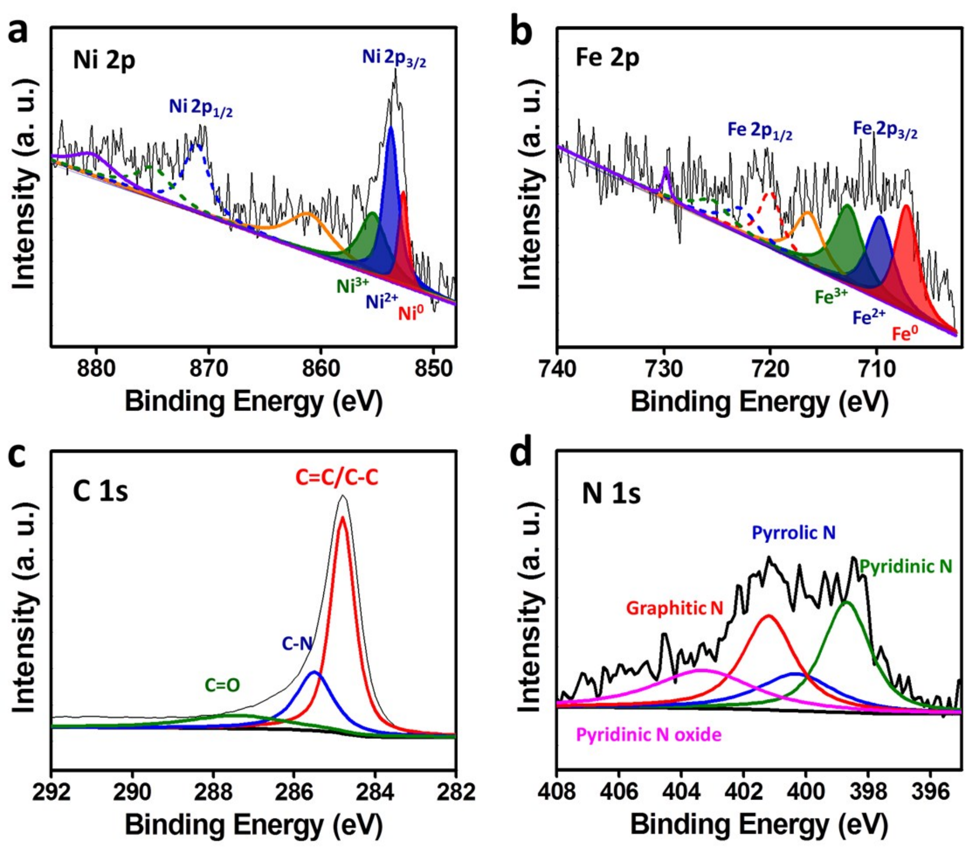

Figure S4. (a) Ni 2p, (b) Fe 2p, (c) C 1s, (d) N 1s XPS Spectra of **FeNi/HNC**.

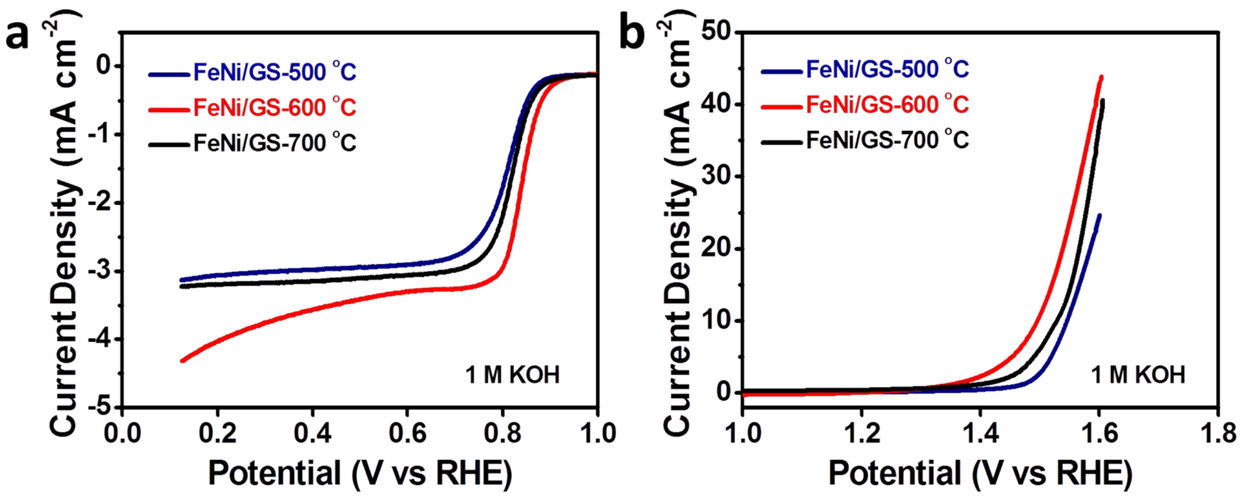

Figure S5. The effect of temperature for the ORR and OER activity for **FeNi/GS** in 1 M KOH.

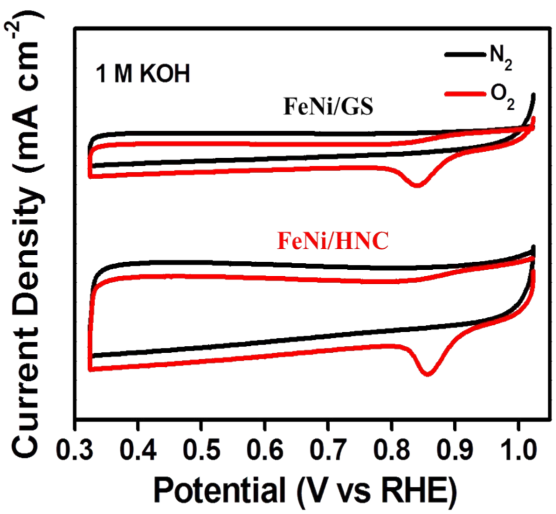

Figure S6. CV curves of **FeNi/GS** and **FeNi/HNC** in 1 M KOH saturated with N_2 (black) or O_2 (red).

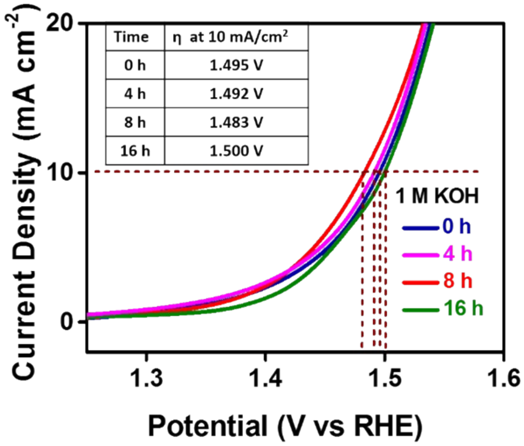

Figure S7. The effect of etching time on OER performance.

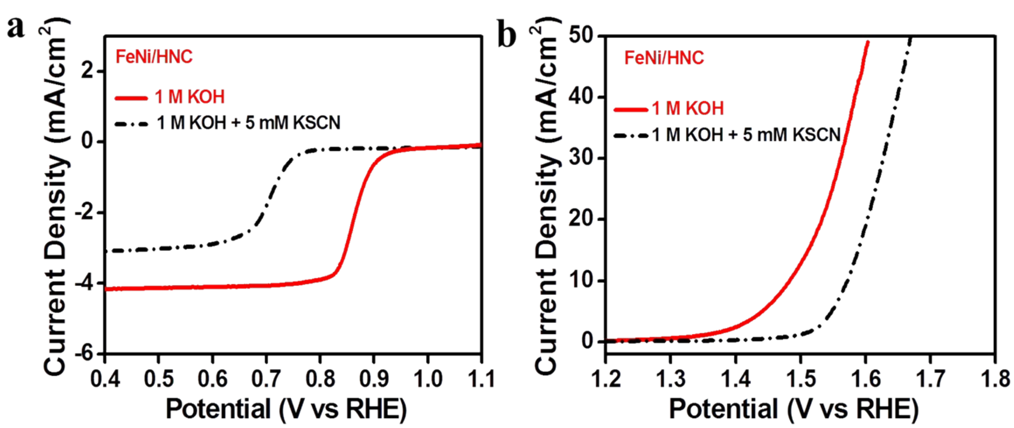

Figure S8. RDE polarization curves of **FeNi/HNC** for the ORR and OER in 1 M KOH (red) and 1 M KOH/5 mM KSCN (black).

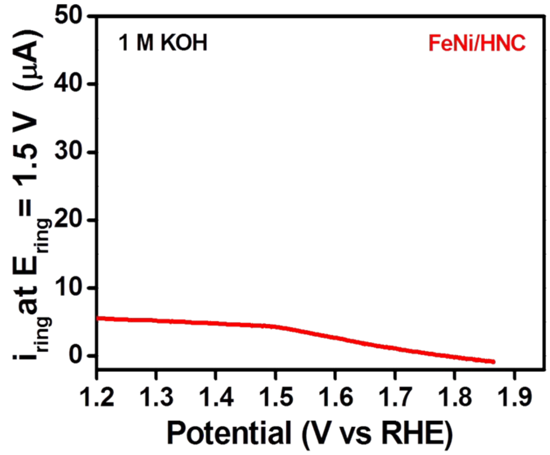

Figure S9. The current of Pt ring at E_{ring}=1.5 V for **FeNi/HNC** during the OER test in 1 M KOH.

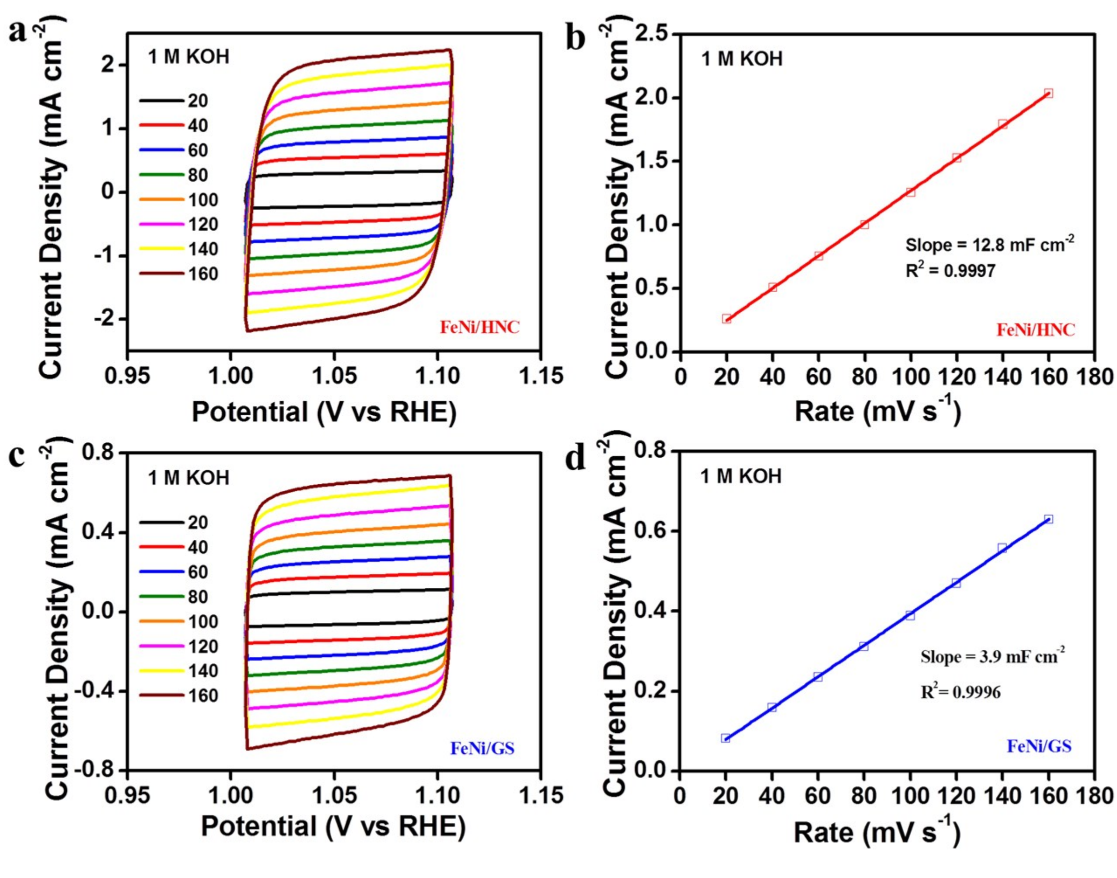

Figure S10. (a and c) CV curves of **FeNi/GS** and **FeNi/HNC** under different scan rates from 20~160 mV s^{-1} in 1 M KOH. (b and d) The plots of capacitive current density at 1.05 V against the scan rate.

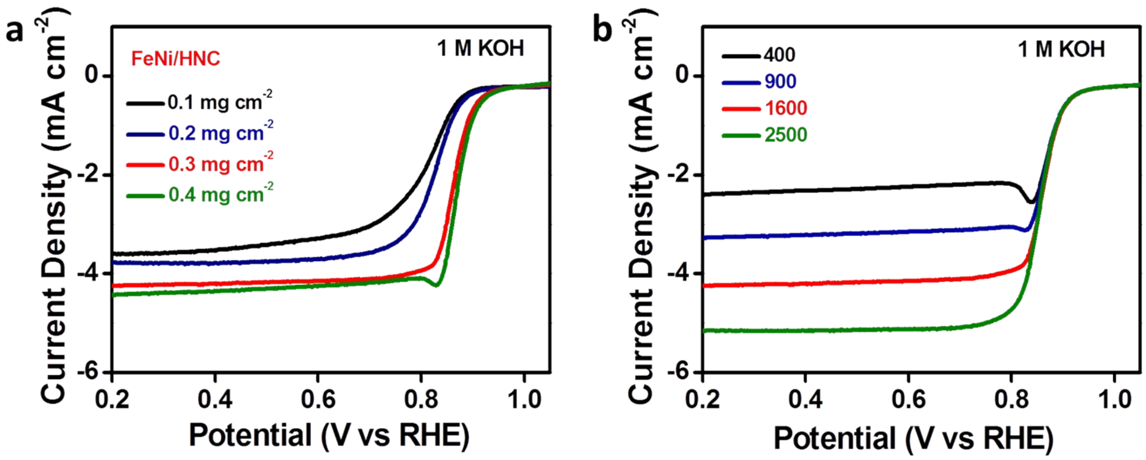

Figure S11. RDE polarization curves of **FeNi/HNC** in O_2-saturated 1 M KOH with different mass loading (a) and at different electrode rotation speeds (b) as noted.

Figure S12. Digital picture of the customized electrochemical cell.

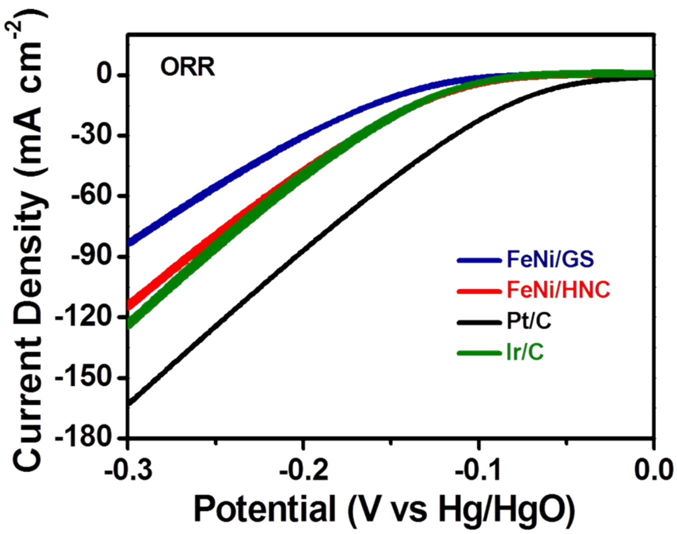

Figure S13. ORR polarization curves of **FeNi/GS**, **FeNi/HNC**, Pt/C and Ir/Cin 6 M KOH. All catalysts have a loading density of 1 mg cm^{-2}.

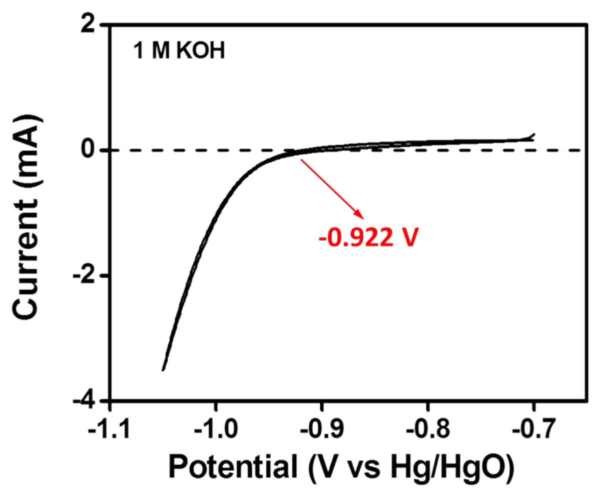

Figure S14. Calibration of Hg/HgO reference electrode with regard to reversible hydrogen electrode (RHE) in a hydrogen saturated electrolyte (1 M KOH), with scan rate 1 mV s^{-1}.

References

1. M. Zeng, Y. Liu, F. Zhao, K. Nie, N. Han, X. Wang, W. Huang, X. Song, J. Zhong and Y. Li, *Adv. Funct. Mater.*, 2016, **26**, 4397-4404.
2. T. Y. Ma, S. Dai, M. Jaroniec and S. Z. Qiao, *J. Am. Chem. Soc.*, 2014, **136**, 13925-13931.
3. D. Chen, C. L. Dong, Y. Zou, D. Su, Y. C. Huang, L. Tao, S. Dou, S. Shen and S. Wang, *Nanoscale*, 2017, **9**, 11969-11975.
4. P. Cai, Y. Hong, S. Ci and Z. Wen, *Nanoscale*, 2016, **8**, 20048-20055.
5. Y. Yang, Z. Lin, S. Gao, J. Su, Z. Lun, G. Xia, J. Chen, R. Zhang and Q. Chen, *ACS Catal.*, 2017, **7**, 469-479.
6. J. Song, C. Zhu, B. Z. Xu, S. Fu, M. H. Engelhard, R. Ye, D. Du, S. P. Beckman and Y. Lin, *Adv. Energy Mater.*, 2017, **7**, 1601555.
7. F. Meng, H. Zhong, D. Bao, J. Yan and X. Zhang, *J. Am. Chem. Soc.*, 2016, **138**, 10226-10231.
8. Y. Ma, X. Dai, M. Liu, J. Yong, H. Qiao, A. Jin, Z. Li, X. Huang, H. Wang and X. Zhang, *ACS Appl. Mater. Interfaces*, 2016, **8**, 34396-34404.
9. X. Cui, P. Ren, D. Deng, J. Deng and X. Bao, *Energ. Environ. Sci.*, 2016, **9**, 123-129.
10. P. Cai, S. Ci, E. Zhang, P. Shao, C. Cao and Z. Wen, *Electrochim. Acta*, 2016, **220**, 354-362.
11. X. Zhao, P. Pachfule, S. Li, J. R. J. Simke, J. Schmidt and A. Thomas, *Angew. Chem. Int. Ed.*, 2018, DOI: 10.1002/anie.201803136.
12. S. Mao, Z. Wen, T. Huang, Y. Hou and J. Chen, *Energ. Environ. Sci.*, 2014, **7**, 609-616.
13. J. Masa, W. Xia, I. Sinev, A. Zhao, Z. Sun, S. Gruetzke, P. Weide, M. Muhler and W. Schuhmann, *Angew. Chem. Int. Ed.*, 2014, **53**, 8508-8512.
14. C. Tang, B. Wang, H. F. Wang and Q. Zhang, *Adv. Mater.*, 2017, **29**, 1703185.
15. P. Chen, T. Zhou, L. Xing, K. Xu, Y. Tong, H. Xie, L. Zhang, W. Yan, W. Chu, C. Wu and Y. Xie, *Angew. Chem. Int. Ed.*, 2017, **56**, 610-614.
16. B. Chen, X. He, F. Yin, H. Wang, D. J. Liu, R. Shi, J. Chen and H. Yin, *Adv. Funct. Mater.*, 2017, **27**, 1700795.
17. G. Fu, Z. Cui, Y. Chen, Y. Li, Y. Tang and J. B. Goodenough, *Adv. Energy Mater.*, 2017, **7**, 1601172.
18. J. Fu, F. M. Hassan, C. Zhong, J. Lu, H. Liu, A. Yu and Z. Chen, *Adv. Mater.*, 2017, **29**, 1702526.
19. L. Wei, H. E. Karahan, S. Zhai, H. Liu, X. Chen, Z. Zhou, Y. Lei, Z. Liu and Y. Chen, *Adv. Mater.*, 2017, **29**, 1701410.
20. G. Fu, Y. Chen, Z. Cui, Y. Li, W. Zhou, S. Xing, Y. Tang and J. B. Goodenough, *Nano Lett.*, 2016, **16**, 6516-6522.
21. L. A. Stern, L. Feng, F. Song and X. Hu, *Energ. Environ. Sci.*, 2015, **8**, 2347-2351.
22. D. Deng, L. Yu, X. Chen, G. Wang, L. Jin, X. Pan, J. Deng, G. Sun and X. Bao, *Angew. Chem.*

Int. Ed., 2013, **52**, 371-375.

23. Y. Liu, H. Jiang, Y. Zhu, X. Yang and C. Li, *J. Mater. Chem. A*, 2016, **4**, 1694-1701.
24. G. Nam, J. Park, M. Choi, P. Oh, S. Park, M. G. Kim, N. Park, J. Cho and J. S. Lee, *ACS Nano*, 2015, **9**, 6493-6501.
25. T. Cao, D. Wang, J. Zhang, C. Cao and Y. Li, *Chem. Eur. J.*, 2015, **21**, 14022-14029.
26. X. Fan, Z. Peng, R. Ye, H. Zhou and X. Guo, *ACS Nano*, 2015, **9**, 7407-7418.
27. B. K. Barman and K. K. Nanda, *Green Chem.*, 2016, **18**, 427-432.
28. Y. Hou, T. Huang, Z. Wen, S. Mao, S. Cui and J. Chen, *Adv. Energy Mater.*, 2014, **4**, 1400337.
29. Z. Y. Wu, X. X. Xu, B. C. Hu, H. W. Liang, Y. Lin, L. F. Chen and S. H. Yu, *Angew. Chem. Int. Ed.*, 2015, **54**, 8179-8183.
30. J. Zhang, Z. Zhao, Z. Xia and L. Dai, *Nat. Nanotechnol.*, 2015, **10**, 444-452.
31. W. Yang, X. Liu, X. Yue, J. Jia and S. Guo, *J. Am. Chem. Soc.*, 2015, **137**, 1436-1439.
32. W. J. Jiang, L. Gu, L. Li, Y. Zhang, X. Zhang, L. J. Zhang, J. Q. Wang, J. S. Hu, Z. Wei and L. J. Wan, *J. Am. Chem. Soc.*, 2016, **138**, 3570-3578.
33. Y. Hou, Z. Wen, S. Cui, S. Ci, S. Mao and J. Chen, *Adv. Funct. Mater.*, 2015, **25**, 872-882.
34. M. Xiao, J. Zhu, L. Feng, C. Liu and W. Xing, *Adv. Mater.*, 2015, **27**, 2521-2527.
35. Y. Hu, J. O. Jensen, W. Zhang, L. N. Cleemann, W. Xing, N. J. Bjerrum and Q. Li, *Angew. Chem. Int. Ed.*, 2014, **53**, 3675-3679.
36. A. Aijaz, J. Masa, C. Roesler, W. Xia, P. Weide, A. J. R. Botz, R. A. Fischer, W. Schuhmann and M. Muhler, *Angew. Chem. Int. Ed.*, 2016, **55**, 4087-4091.
37. X. Liu, M. Park, M. G. Kim, S. Gupta, G. Wu and J. Cho, *Angew. Chem. Int. Ed.*, 2015, **54**, 9654-9658.
38. J. Wang, H. Wu, D. Gao, S. Miao, G. Wang and X. Bao, *Nano Energy*, 2015, **13**, 387-396.
39. M. Wang, T. Qian, J. Zhou and C. Yan, *ACS Appl. Mater. Interfaces*, 2017, **9**, 5213-5221.
40. M. Wang, T. Qian, S. Liu, J. Zhou and C. Yan, *ACS Appl. Mater. Interfaces*, 2017, **9**, 21216-21224.
41. H. Wu, J. Wang, G. Wang, F. Cai, Y. Ye, Q. Jiang, S. Sun, S. Miao and X. Bao, *Nano Energy*, 2016, **30**, 801-809.
42. Y. Su, Y. Zhu, H. Jiang, J. Shen, X. Yang, W. Zou, J. Chen and C. Li, *Nanoscale*, 2014, **6**, 15080-15089.
43. G. L. Tian, M. Q. Zhao, D. Yu, X. Y. Kong, J. Q. Huang, Q. Zhang and F. Wei, *Small*, 2014, **10**, 2251-2259.
44. Y. Li, M. Gong, Y. Liang, J. Feng, J. E. Kim, H. Wang, G. Hong, B. Zhang and H. Dai, *Nat. Commun.*, 2013, **4**, 1805.
45. J. S. Lee, T. Lee, H. K. Song, J. Cho and B. S. Kim, *Energ. Environ. Sci.*, 2011, **4**, 4148-4154.
46. J. S. Lee, G. S. Park, H. I. Lee, S. T. Kim, R. Cao, M. Liu and J. Cho, *Nano Lett.*, 2011, **11**,

5362-5366.

47. S. Zhu, Z. Chen, B. Li, D. Higgins, H. Wang, H. Li and Z. Chen, *Electrochim. Acta*, 2011, **56**, 5080-5084.

48. Z. Chen, J. Y. Choi, H. Wang, H. Li and Z. Chen, *J. Power Sources*, 2011, **196**, 3673-3677.

49. G. S. Park, J. S. Lee, S. T. Kim, S. Park and J. Cho, *J. Power Sources*, 2013, **243**, 267-273.

50. Z. Li, M. Shao, Q. Yang, Y. Tang, M. Wei, D. G. Evans and X. Duan, *Nano Energy*, 2017, **37**, 98-107.

51. X. Han, X. Wu, C. Zhong, Y. Deng, N. Zhao and W. Hu, *Nano Energy*, 2017, **31**, 541-550.

52. Q. Liu, Y. Wang, L. Dai and J. Yao, *Adv. Mater.*, 2016, **28**, 3000-3006.

53. S. S. Shinde, C. H. Lee, A. Sami, D. H. Kim, S. U. Lee and J. H. Lee, *ACS Nano*, 2017, **11**, 347-357.

54. Z. Cui, G. Fu, Y. Li and J. B. Goodenough, *Angew. Chem. Int. Ed.*, 2017, **56**, 9901-9905.

55. X. Liu, M. Park, M. G. Kim, S. Gupta, X. Wang, G. Wu and J. Cho, *Nano Energy*, 2016, **20**, 315-325.